CHARACTERIZATION OF ORBITAL DEBRIS VIA HYPER-VELOCITY LABORATORY-BASED TESTS

Heather Cowardin[(1)], J.-C. Liou[(2)], Phillip Anz-Meador[(3)], Marlon Sorge[(4)], John Opiela[(3)], Norman Fitz-Coy[(5)], Tom Huynh[(6)], Paula Krisko[(3)]

[(1)] University of Texas-El Paso, Jacobs JETS Contract, NASA Johnson Space Center
2224 Bay Area Blvd, Houston, TX 77058, USA, heather.cowardin@nasa.gov
[(2)] NASA Orbital Debris Program Office, NASA Johnson Space Center,
2101 NASA Parkway, Houston TX 77058, USA, jer-chyi.liou-1@nasa.gov
[(3)] Jacobs, NASA Johnson Space Center, 2224 Bay Area Blvd, Houston, TX 77058, USA
phillip.d.anz-meador@nasa.gov, paula.krisko-1@nasa.gov and john.n.opiela@nasa.gov
[(4)] The Aerospace Corporation, 2155 Louisiana Blvd. NE #5000, Albuquerque, NM 87110, USA marlon.e.sorge@aero.org
[(5)] University of Florida, nfc@ufl.edu
[(6)] Air Force Space and Missile Systems Center 483 North Aviation Blvd., El Segundo, CA 90245, USA,
thomas.huynh@us.af.mil

ABSTRACT

Existing DOD and NASA satellite breakup models are based on a key laboratory test, Satellite Orbital debris Characterization Impact Test (SOCIT), which has supported many applications and matched on-orbit events involving older satellite designs reasonably well over the years. In order to update and improve these models, the NASA Orbital Debris Program Office, in collaboration with the Air Force Space and Missile Systems Center, The Aerospace Corporation, and the University of Florida, replicated a hypervelocity impact using a mock-up satellite, DebriSat, in controlled laboratory conditions. DebriSat is representative of present-day LEO satellites, built with modern spacecraft materials and construction techniques. Fragments down to 2 mm in size will be characterized by their physical and derived properties. A subset of fragments will be further analyzed in laboratory radar and optical facilities to update the existing radar-based NASA Size Estimation Model (SEM) and develop a comparable optical-based SEM.

A historical overview of the project, status of the characterization process, and plans for integrating the data into various models will be discussed herein.

1 INTRODUCTION/MOTIVATION

The DebriSat project is a collaboration of the NASA Orbital Debris Program Office (ODPO), the Air Force Space and Missile Systems Center (SMC), The Aerospace Corporation (Aerospace), the University of Florida (UF), and the Air Force Arnold Engineering Development Complex (AEDC). The project has four primary goals: 1) design and fabricate a 56-kg class spacecraft ("DebriSat") representative of modern spacecraft in the low Earth orbit (LEO) environment; 2) conduct a hypervelocity laboratory impact test to simulate a catastrophic fragmentation event on DebriSat; 3) collect, measure, and characterize all fragments down to 2 mm in size; and 4) use the data to improve space situational awareness applications and satellite breakup models for better orbital debris environment definition [1].

The motivation for the DebriSat project was based on a key impact test series, Satellite Orbital Debris Characterization Impact Test (SOCIT), which was conducted by the Department of Defense (DOD) and NASA at AEDC in 1992 to support the development of satellite breakup models. The main target for SOCIT was a fully functional U.S. Navy Transit 1960's era satellite. The DOD and NASA breakup models based on the SOCIT data have supported many applications and matched on-orbit events reasonably well over the years [1].

As new materials and construction techniques are developed for modern satellites; however, there is a need for new laboratory-based tests to acquire data to improve the existing DOD and NASA breakup models. The need for such tests is supported also by discrepancies between model predictions and observations of fragments generated from the breakup of modern satellites, including the Iridium 33 and Fengyun 1-C [2].

The DebriSat design was based on a survey of modern satellites in LEO [3, 4]. All major design decisions, including the selection of components, subsystems, mass fractions, structure, and construction methods were

Proc. 7th European Conference on Space Debris, Darmstadt, Germany, 18–21 April 2017, published by the ESA Space Debris Office
Ed. T. Flohrer & F. Schmitz, (http://spacedebris2017.sdo.esoc.esa.int, June 2017)

reviewed and approved by Aerospace subject matter experts. In addition, the DebriSat body was covered with multi-layer insulation (MLI) and three solar panels were attached to one side of the main body (Fig. 1, 2).

To reduce the project cost, a decision was made to emulate the majority of components. The emulated components were based on existing designs of flight hardware, including structure, dimensions, materials, and connection mechanisms. At the end of the assembly, DebriSat was subjected to a NASA General Environmental Verification Specification qualification vibration test to ensure the integrity of the structure.

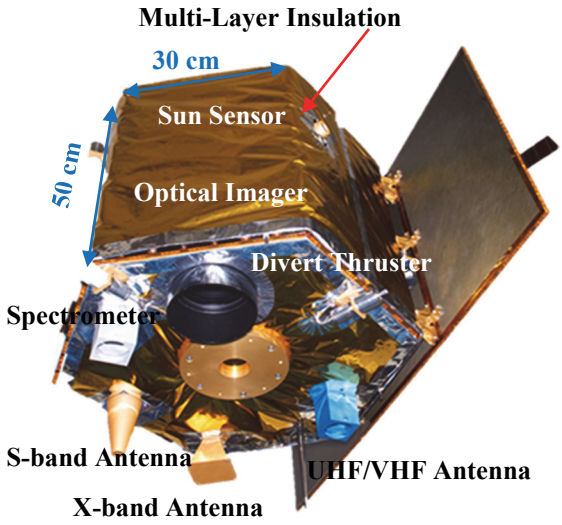

Figure 1. DebriSat Design

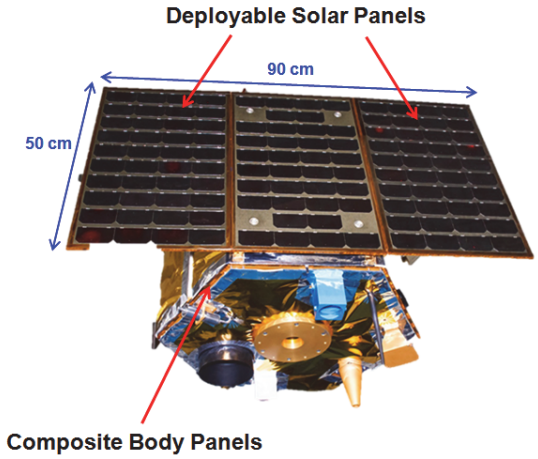

Figure 2. DebriSat Design

To increase the project's benefits further, Aerospace designed and built a target resembling a launch vehicle upper stage ("DebrisLV") for the pre-test shot. Fig. 3 shows the mounting of DebrisLV inside the target chamber.

Figure 3. DebrisLV mounted inside impact chamber

Another key element that was implemented in DebriSat and DebrisLV hypervelocity impact tests was the use of a soft catch system inside the chamber to capture fragments and minimize secondary damage to fragments due to contact with the walls of the test chamber. In the SOCIT test series the foam catch system, which consisted of panels, was used only in the downrange and sideways directions. Based on the experiences from the SOCIT impact test, the DebriSat project increased the thickness of the soft-catch foam panels and the interior of the target chamber was fully covered with these soft-catch foam panels to prevent any fragments from impacting the chamber walls, which would produce secondary damage not associated with the breakup. Tab. 1 shows a comparison of some SOCIT, DebriSat, and DebrisLV test conditions.

2 DEBRISAT BACKGROUND

From 2009-2014 the planning and fabrication for the DebriSat and DebrisLV were in process. On 1 April and 15 April 2014, respectively, the DebrisLV and DebriSat impacts were successfully carried out at AEDC Range G. Range G operates the largest two-stage light gas gun in the United States. To maximize the projectile mass at the 7 km/sec impact speed, the AEDC team developed a special projectile design featuring a hollow aluminum cylinder embedded in a nylon cap, which did not require a sabot. The nylon cap served as a bore rider for the aluminum cylinder to prevent hydrogen leakage and to protect the barrel [1].

Table 1. SOCIT, DebriSat, & DebrisLV Comparison

	SOCIT/ Transit	DebriSat	DebrisLV
Target body dimensions	46 cm (dia) × 30 cm (ht)	60 cm (dia) × 50 cm (ht)	35 cm (dia) × 88 cm (ht)
Target mass	34.5 kg	56 kg	17.1 kg
MLI and solar panel	No	Yes	No
Projectile material	Al sphere	Hollow Al cylinder with attached nylon bore-rider	Hollow Al cylinder with attached nylon bore-rider
Projectile dimension/mass	4.7 cm diameter, 150 g	8.6 cm × 9 cm, 570 g	8.6 cm × 9 cm, 598 g
Impact speed	6.1 km/sec	6.8 km/sec	6.9 km/sec
Impact Energy to Target Mass ratio (EMR)	81 J/g (2.8 MJ total)	235 J/g (13.2 MJ total)	832 J/g (14.2 MJ total)
Soft-Catch System: Polyurethane foam stacks	3 densities: 0.06, 0.096, and 0.192 g/cm3; 25 cm thick	3 densities: 0.048, 0.096, and 0.192 g/cm3; up to 61 cm thick	3 densities: 0.048, 0.096, and 0.192 g/cm3; up to 51 cm thick

After the impacts of DebrisLV and DebriSat, all intact foam panels, broken foam pieces, loose fragments, and dust were carefully collected, processed, documented, and placed in bags or plastic containers for shipping to a storage facility. The initial estimates using the NASA Breakup Model indicated the number of 2 mm (and larger) fragments from DebriSat and DebrisLV were approximately 85,000 and 35,000, respectively. In total, 41 pallets (~2 × 2 × 2 m) of boxes were packed for both tests and sent to UF for the next step in the process: to collect, measure, and characterize all fragments down to 2 mm in size.

Since 2014, the UF team has been working to extract fragments from foam panels, characterize each fragment down to 2 mm in size, and upload the data into a database. The details and status of the characterization process will be discussed in Section 3.0.

3 FRAGMENT CHARACTERIZATION

The project's primary goal is to recover at least 90% of the total DebriSat mass from the fragments and to measure the physical properties of all recovered fragments. To achieve this goal, all fragments with at least one dimension ≥2 mm are carefully collected and/or extracted from the foam panels/pieces and assigned unique identification numbers before their physical characteristics are measured. A priority of the characterization process is to develop and implement methodologies to minimize biases and/or errors associated with "human-in-the-loop" activities during measurements. The overall process flow is shown in Fig. 4.

During the characterization process, each fragment's physical (observed and derived) parameters are archived in the DebriSat Categorization System (DCS). The DCS is a database solution designed and developed specifically to manage the large amounts of data generated by the DebriSat project. The list of parameters is shown in Tab. 2. In addition to the information shown in Tab. 2, associated metadata (*e.g.*, location the fragment was found within the chamber, images of the fragments, etc.) are also archived in the DCS.

3.1 Post Impact Process

The first step of the post-impact process involves detecting the objects. For fragment detection each foam panel (soft catch) is prepared for X-ray image acquisition by collecting loose and embedded fragments on the surfaces of the panels. Once preparation is completed, the panels are X-rayed and the X-ray images post-processed to detect embedded fragments. [5].

The second step is fragment extraction, which involves recovery of embedded fragments from the panels utilizing results from the X-ray images. Prior to this step, each panel is verified to ensure that the preparation data is properly entered into the DCS. Then fragments with at least one dimension greater than 2 mm are carefully extracted and recorded into the DCS and given unique identification numbers and barcodes. Due to the large amount of data associated with each individual debris fragment, multiplied by the massive number of debris, the use of unique identification numbers and barcodes is critical in the characterization process. By utilizing unique identifiers, each fragment's data can be accessed and retrieved from the DCS any time during post-impact processing and analysis [5, 6].

Table 2. Fragment parameters captured in database

Parameter	Definition/Notes
Unique ID with associated barcode	Earlier studies grouped multiple, similar small fragments to get average characteristics
Material	Predefined categories based on as-built design; material density is auto-populated once material is selected.
Shape	1. Flat Plate 2. Bent Plate 3. Straight Needle/Rod/Cylinder 4. Bent Needle/Rod/Cylinder 5. Parallelepiped/Nugget/Spheroid 6. Flexible/MLI
Color	Predefined categories based on as-built design
Principle dimensions	x, y, z (mm)
Characteristic length	$L_c = {(x+y+z)}/{3}$ (mm)
Average cross-sectional area	Weighted average of projected areas visible in multiple 2-D images; pixel-to-length (and area) relationship calculated from hardware characteristics and scene geometry (mm^2).
Mass	Fragment mass (g)
Area-to-mass ratio (AMR)	Calculated average cross-sectional area divided by measured mass (mm^2/g).
Volume	Calculated from point cloud using convex hull and alpha-shape subtraction (mm^3).
Bulk Density	Measured mass divided by calculated volume (g/mm^3).

The characterization process is broken into three major categories: Assessment, Measurement, and Calculation, as shown in Fig. 4. [5]. The initial step in the characterization process involves assessing each uniquely identified fragment in terms of material, shape, color, and what imaging system the fragment qualifies for: two dimensional (2D) or three dimensional (3D) imaging. The 2D imaging system is primarily designed for flat objects, those with a third dimension (height) that is negligible in comparison to the other two dimensions. The 3D imager is for larger objects that do not meet the 2D imager threshold. The 3D system requires more time than the 2D system for data acquisition. Details of the two imaging systems will be discussed next.

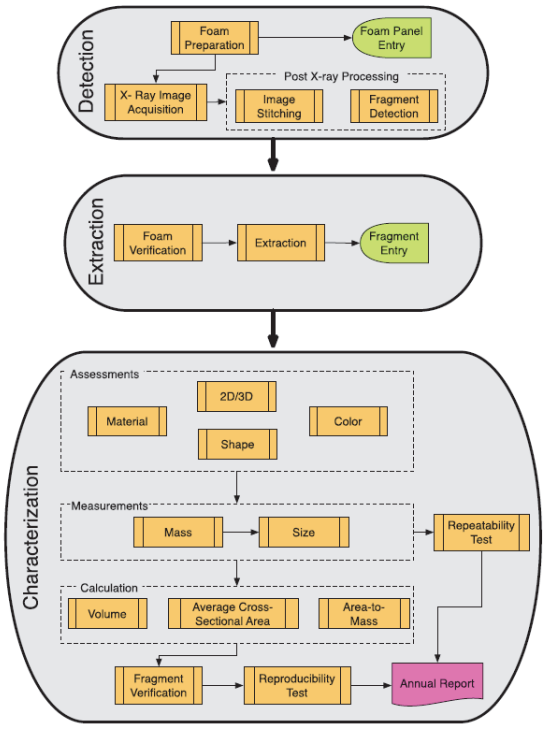

Figure 4. Post-impact Process Flow Diagram

The 2D measurement process involves computing the two largest in-plane dimensions using a single 2D image acquired by the 2D imaging system, see Fig. 5. The 2D imaging system consists of a single Canon PowerShot S110 camera, an imaging platform with LED lights controlled by an Arduino, a barcode scanner, a shroud, and a computer with the 2D imaging GUI. The shroud serves two purposes: it blocks external light and minimizes air perturbations that may cause the fragment to move during the imaging process. [5]

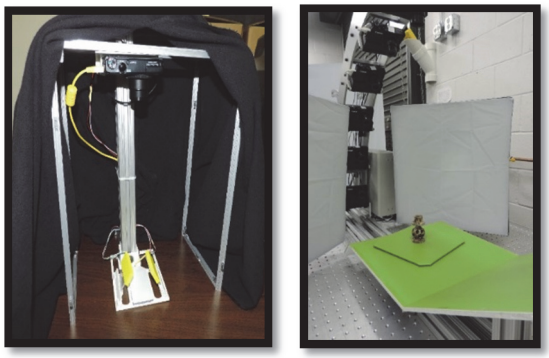

Figure 5. 2D imager (left) 3D imager (right)

Fragments that have been categorized as 3D objects from the size assessments are processed using the 3D imaging system. The 3D imaging system, shown on the right in Fig. 5, consists of six point-and-shoot cameras, a green-screen turntable controlled by an Arduino, three light boxes, and a computer with the 3D-imaging GUI. The six cameras are distributed (18 degrees apart) along a vertical arch providing varied elevations relative to the fragment. The turntable rotates the object through multiple azimuths for a full 360-degree view of the object. Three-dimensional processing involves constructing a 3D representation from multiple camera images utilizing a space carving technique. Images are acquired from fixed azimuth and elevation angles around the object to provide the data needed for the 3D reconstruction. A checkerboard calibration pattern is used to identify the camera parameters, such as orientation, position, focal length, and others. From the camera parameters, the pixel-to-millimeter ratio is computed and used in the size measurement. [5]

3.2 Characterization Status

A summary of the status of the characterization process is shown below.

Table 3. Status of post-impact process

Panels prepped for X-ray	375/564
Panels X-rayed	298/564
Panels extracted	198/564
Fragments collected (estimate)	142,000
Fragments recorded in DCS	132,418
Fragments Characterized	9400
Fragments Verified	453

From 2016-2017 the focus for the characterization process was on the small carbon fiber reinforced polymer (CFRP) fragments. They were ideal for the 2D imager, which was already verified and met the criteria for 2D imaging due to their small sizes and generally flat shapes. The material density was well known, thus a third dimension could be derived from the material density and area measurements. In November 2016, it was decided to move forward with calibrating and verifying the 3D imager and implementing a mirror in the 2D imager to directly measure the fragments' third dimension. As of late February 2017, work was on going with the 2D imager software to extract height, and to characterize the 3D imager to eliminate any systematic biases that may propagate into the size calculations.

4 PLANS FOR LABORATORY-BASED ANALYSIS

To better characterize the data acquired from ground-based measurements, specifically optical and radar assets, laboratory-based measurements and analysis provide a means to assess a fragment's known size, shape, material characterization, and to provide insight into remote detection of fragments in the optical and radar regime. One of the objectives for continued analysis of the DebriSat fragments is to select a number of representative fragments to use as targets in laboratory facilities. The following will provide background on optical and radar laboratory-based measurements and how the data will be used to create and update size estimation models.

4.1 Optical

Optical observations of orbital debris provide time-dependent photometric data that yield lightcurves in multiple bandpasses, which aid in material identification and possible periodic orientations. These data can also be used to help identify shapes and optical properties at multiple phase angles. Capitalizing on optical data products and applying them to generate a more complete understanding of orbital space objects is a key objective of NASA's Optical Measurements Program and a primary objective for the creation of the Optical Measurements Center (OMC). The OMC is used to emulate space-based illumination conditions using equipment and techniques that simulate telescopic observations and source-target-sensor orientations. The design of the OMC is analogous to a telescope set-up with a light source, target, and observer. A 75-watt, Xenon arc lamp simulates solar illumination through the spectral range of 200 to 2500 nm. The data are acquired through a Santa Barbara Instrument Group CCD camera (1024 x 1536 pixels) with an attached filter wheel that uses either the standard Johnson/Bessell (blue, visible, red, and infrared) or Sloan Digital Sky Survey (g',r',i',z'-band) astronomical filter suite. Spectral measurements are also employed to baseline various material types using a quartz lamp as an illuminator and an Analytical Spectral Device field spectrometer (range from 300-2500 nm). Instrumentation layout is shown in Fig. 6.

The OMC will be used to provide optical measurements on a subset of DebriSat fragments to acquire empirical bidirectional reflectance distribution function (BRDF) measurements. BRDF measurements allow a proper sampling of the target's response in each selected band and phase angle over a 2π steradian angular range. These measurements eliminate the need to know the exact

aspect angle of targets relative to ground-based sensors, and provide a reflectance distribution for all aspect angles for the target.

During the fabrication/construction phase of the DebriSat project, spectral measurements were acquired on the majority of DebriSat and DebrisLV materials to baseline the spectral response. Spectral measurements will be conducted on selected fragments of known material to compare pre- and post-impact reflectance measurements, which will aid in a better understanding of how materials and their respective albedo measurements potentially vary during in-orbit fragmentation events.

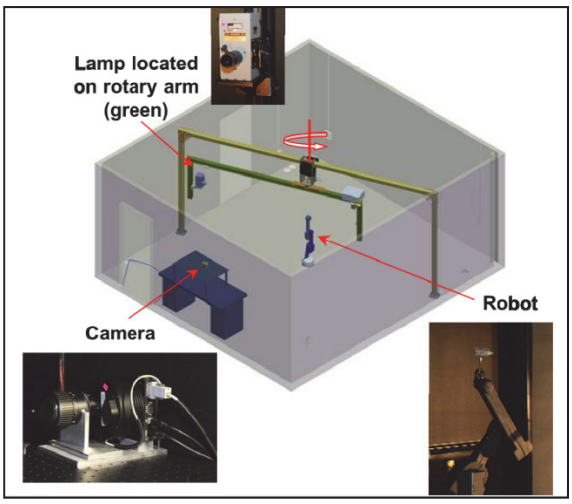

Figure 6. Overhead view of OMC with primary instrumentation.

The goal of these measurements will be to provide an optical size estimation model (OSEM), eliminating the need for the current assumptions used to determine an object's physical cross section, a sphere with diameter (d), see Eq. 1. The size dimension assumes a distance or range (R); for instance, objects observed in the GEO region would have R=36,000 km. The geometrical albedo, A_g, of the target's surface is defined as one value (0.175) [7]. The phase function, Ψ (α), defines how the sunlight is scattered by the surface in a direction α to the observer. The two primary phase functions are Specular (independent of the scattering angle) and diffuse Lambertian. Details of the size calculation based on optical measurements are provided by Barker, *et al.* [8],

$$d = \frac{2 \cdot R}{[\pi \cdot A_g \cdot \Psi(\alpha)]^{0.5}} \cdot 10^{\left[\frac{Mabs(v)+Msun(v)}{-5.0}\right]} \quad (1)$$

One of the objectives of the laboratory measurements is to use the spectral response to investigate albedo variations dependent on various processes that can change a material's reflectivity, including but not limited to: space-environment aging in various orbital regimes and effects from impact experiments (such as DebriSat) at various chamber pressures. The OMC laboratory-based measurements will be used to better define an albedo distribution, rather than the current estimate that assumes one value for all materials in all orbits, as well as to investigate other phase functions that correlate with the laboratory data analysis.

Using the BRDF measurements acquired at a known range (distance from sensor to target), phase angle (source-target-sensor angle), and albedo distribution, an OSEM can be developed to better assess the size of uncorrelated targets in Earth orbit that represent the majority of the orbital debris population.

4.2 Radar

The MIT/LL HUSIR and HAX radar systems have been in use since the early 1990s to observe the orbital debris environment using staring mode operations. The data collected are used to estimate the range, range-rate, and derived radar cross section (RCS) of objects. The RCS is defined as the measure of reflective strength using 4π times the ratio of the power per unit solid angle in the scattered wave (E_{scat}) as a function of the power per unit area of the illuminated beam (E_{int}), shown in Eq. 2:

$$\sigma = \lim_{r \to \infty} 4\pi r^2 \frac{|E_{scat}|^2}{|E_{int}|^2}, \quad (2)k$$

where r relates to the distance from the scatterer to the point where the scattered power is measured [9]. Both E_{scat} and E_{int} are complex field amplitudes at any point in space and are dependent upon the arrival of the incident wave in relation to the direction of the scattered wave [10, 11]. The scattering angle is defined by the transmitter and receiver locations, similar to phase angle. This scattering angle defines bistatic (transmitter and receiver at different locations) and the monostatic (transmitter and receiver are collocated, scattering angle equals 180°) RCS values. The RCS of an object is a complex combination of multiple factors such as size, material, shape, and the spatial orientation of the object, as well as wavelength and polarization of the incident wave [12]. These complexities hinder the direct correlation between an object's physical size and RCS measurement. Objects of the same shape may have dramatically different scattering behaviors, given different materials. For a perfectly conducting sphere (conductivity→∞ and both real and imaginary parts of the refractive index→∞), the

backscattering properties are well known and documented. In the Rayleigh region the wavelength dependence of the RCS for a sphere is proportional to λ^{-4} (*i.e.,* size << λ). The optical regime refers to cases when sphere size is much larger than wavelength. For metallic spheres in the optical regime, the RCS is independent of wavelength and directly related to physical cross section, πa^2, where 'a' is the radius of the sphere [13]. Within the resonance region there are two contributions that form constructive and destructive interference waves, one from the specular reflection from the front of the sphere and one from the creeping wave that travels around the back of the sphere and returns to the incident radar, interfering with the reflection from the front of the sphere [15]. For non-spherical objects the RCS becomes more complicated depending on an object's shape and spatial orientation, in addition to size, material composition, aspect angle (mono-static versus bi-static) and polarization. For a very long, thin homogenous wire the mono-static RCS will vary as a function of orientation. The RCS signal will be the greatest when the longest dimension is normal to the incident beam, as expected in optical scattering theory, except that as the apparent size decreases (away from the longest dimension) the backscatter levels off followed by an increase in backscatter.

To address the complexities of RCS measurements due to size, shape, and composition, an indoor radar range was contracted to measure the RCS of a selected set of fragments in comparison to physical size. The physical measurements (characteristic length (L_c), area, and mass) were taken using calipers, a standard ruler, and a laboratory scale. The L_c was determined to best represent the diameter of an object by averaging the three projected dimensions of any shape based on RCS data, which is true for a sphere. This parameter also defines the median area one would expect to measure as an object tumbles or rotates in space. The majority of the objects collected were aluminum or steel. The radar measurements were taken at multiple angles in order to avoid undersampling the RCS angle variations. This type of sampling is very similar to the measurement technique used in the OMC. The data also were taken at a wide range of frequencies from 2.4 to 18 GHz (covering the S, C, X and Ku bands), which also are equivalent radar bands used for orbital debris tracking and detection.

The measured RCS parameter ($z = RCS/\lambda^2$) and physical size parameter ($x = size/\lambda$) were plotted as a function of multiple viewing angles to determine a scaling curve to represent the mean of the measured RCS for each size/wavelength (shown in Fig. 7). The mean of the RCS parameter for each size parameter results in a smooth scaling curve that defines the basis of the NASA size estimation model (SEM) [12, 16]. This model provides a simple one-to-one relationship between RCS and physical size, given a radar wavelength [12, 16].

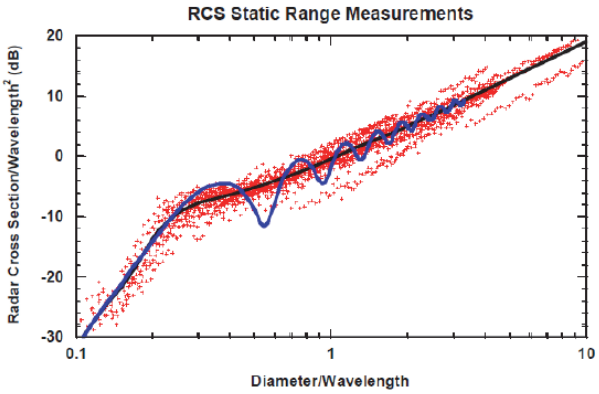

Figure 7. Plot of RCS/wavelength^2 versus diameter/wavelength taken from radar range. Blue line symbolizes perfectly conducting sphere.

One of the goals for the DebriSat project is to reassess the SEM using a subset of chosen fragments (same subset used for the OMC analysis). This will involve measuring RCS of the fragments through a number of different wavelengths and orientations similar to the 1993 experiment. DebriSat fragments will include more modern-day spacecraft materials and enable a larger sample size. The RCS vs. size relationship will also be thoroughly compared with the derived optical size parameter to better define the target's size in the two wavelength (frequency) regimes.

5 DATA INTEGRATION INTO BREAKUP MODELS

The NASA and DOD orbital debris modeling efforts have been generally independent though parallel. Each program maintains its own fragmentation models and its own database of orbiting objects and their physical characteristics. Both models are used for many of the same basic purposes including long-term debris environment modeling and short-term satellite risk assessments. Although they have similar uses, details of the motivations for their developments have led to somewhat different approaches in the specifics of the models. The NASA model is the SSBM (Standard Satellite Breakup Model) [17]. It was developed and is maintained by the ODPO. The DOD model, IMPACT [18], was developed and is maintained by The Aerospace Corporation. Both groups share and support the impact databases of SOCIT and DebriSat. Comparisons between the two models and actual fragmentation data

demonstrate good matchups for the parameters of mass, L_c, and spreading velocity.

Other parameters of interest by both NASA and DOD models include the fragment's area-to-mass ratio (AMR), material, and effective density. These parameters affect the way that debris fragment orbits evolve, and the potential lethality of the fragments in an impact with a satellite. In spite of differences in modeling approaches, the results from both models are frequently similar across different fragmentation event parameters. For example, one of the important characteristics of debris fragments is their AMR, as this parameter determines the evolution of the fragments' orbits over time. The AMR is a function of the area, a size and shape-related parameter, and mass. This again emphasizes the importance of the size-shape-mass relationships that characterize fragmentation debris in the understanding of its evolution over time. It is particularly important to have accurate AMR models for debris below the SSN trackable threshold (*i.e.*, smaller than 10 cm in LEO) as it is not possible to directly compare modeled results to actual.

Over the years these parameters have been gleaned by careful study of successive ground test data from impact tests. The most important such test to date for both SSBM and IMPACT is the SOCIT impact test discussed in Section 1. It was the culmination of a number of impact ground-based tests that showed the effect of a small impactor on an actual satellite at orbiting speeds. The fragments were available for scrutiny. Ten fragment parameters, (excluding spreading velocity); the mass, L_c, size, shape, AMR, materials, volume, area, and effective density have been cataloged and analyzed.

5.1 The NASA SSBM

The NASA Standard Satellite Breakup Model (SSBM) [17] was formulated using laboratory tests and ground-based remote measurements of on-orbit fragmentation events to provide an average breakup ensemble for spacecraft and upper stage collisions and explosions. The motivation for developing the SSBM was two-fold: the availability of new radar, optical, and *in situ* environmental measurements in the late 1980s and early-to mid-1990s; and a thorough review of the performance of the then-current breakup model, as used in EVOLVE 3.0, NASA's long-term Monte Carlo environment simulation computer program. Measurements of the environment invalidated certain early data sets and concepts based on those data, *e.g.*, "high-" and "low-intensity explosions." Measurements also revealed discrepancies between simulated and actual outcomes, attributable to the manner in which the mass-to-size conversion and the single-valued AMR were modeled. The SSBM was developed in a systematic manner by examining all available, relevant data—it is a data-driven model. Following significant validation efforts against observable data, the SSBM was deployed in EVOLVE 4.0 and serves the same role with EVOLVE's successor, the LEO to GEO Environment Debris 3D long-term environment model (LEGEND) [17].

The SSBM uses L_c as the fundamental independent variable in lieu of the preceding model's use of mass. This choice of L_c in preference to mass was driven by the on-orbit observables, namely Two Line Element (TLE) orbital data sets and radar cross section (RCS) time series. The TLE sets provide sufficient information to determine or infer number of fragments and their post-event orbits, the AMR, and separation velocities for members of specific breakup event ensembles. The RCS time series provide sufficient information to infer L_c and area. Orbital data was used to derive and validate distributions for $L_c > 11$ cm. Laboratory data, including the SOCIT [19] and the ESA Ariane subscale model explosion series, were essential in defining the distributions below approximately 8 cm, and a bridging function spans the 8-11 cm L_c gap. Distributions in cumulative number, area, and AMR for collision and explosion fragments are provided by the SSBM; the cumulative number distribution for collisions additionally incorporates mass characteristics of the event to model catastrophic and non-catastrophic collisions. The separation velocity (Δv) distribution uses AMR as its independent variable. Mass of a given object is calculated as the quotient of area and AMR.

A major departure from the SSBM was the partitioning of the SSBM ensemble functions by mass density. This was done by integrating SOCIT density data into three density categories [20] for fragments between 1 mm and 10 cm in L_c (objects larger than 10 cm are assigned the nominal density of 2.8 g/cm^3). The motivation for this SSBM variant was to facilitate development of the NASA Orbital Debris Engineering Model (ORDEM) 3.0. The density categories are low density (< 2.0 g/cm^3, including 0.9 g/cm^3 sodium-potassium coolant droplets, nominal density 1.4 g/cm^3), medium density (2.0 g/cm^3 to 6.0 g/cm^3, nominal density 2.8 g/cm^3) and high density (> 6.0 g/cm^3, nominal density 7.9 g/cm^3). AMR is monitored to ensure that a given statistical draw from the distribution does not result in an object more dense than is realizable in a given category—the consequence of which would be unrealistically long orbital lifetimes. The ORDEM 3.0 and NASA BUMPER II impact risk model experience is that the high- and medium-density

categories pose the principal risk to resident space objects.

The NASA Engineering Safety Center (NESC) provided guidance for the ORDEM update that resulted in the deployment of ORDEM 3.0. The inclusion of density as a parameter was accomplished in ORDEM 3.0; however, the NESC recommendation that shape be included in the breakup ensemble has been deferred to ORDEM 4.0. Analysis of the DebriSat and DebrisLV datasets will figure prominently in extending the density distribution from three categories to the effective density distribution and incorporating, for the first time, shape effects.

5.2 The Aerospace IMPACT Model

The IMPACT fragmentation model was initially developed in the mid-1980s to predict the risks to satellites from on-orbit fragmentation events. The model underwent significant modifications in the early 1990s based on the availability of additional ground test data, such as the SOCIT test, as well as data from on-orbit fragmentation events.

IMPACT is a mass-based, semi-empirical model combining empirical distributions for parameters such as number, spreading velocity, fragment dimensions, and AMR, with physical conservation laws and boundary conditions. The linking of the empirical relationships to conservation laws prevents the collective results of the empirical relationships from exceeding realistic limits and provides a means to link the behavior of the different empirical expressions together.

IMPACT's initial focus on modeling the characteristics of individual fragmentation events motivated the inclusion of very basic material property considerations into the relationships between fragment, mass size, and AMR. This enabled the model to recreate material-based fragment characteristic differences that had been observed in ground test data. It also enabled modeling of fragmentation events where the objects contained significant quantities of unusual materials.

Another effort to refine IMPACT occurred during the late 2000s, when over 11,000 pieces of debris from more than three-dozen historical on-orbit fragmentation events were characterized. The results of this characterization effort were compared to IMPACT predictions to refine model sub-components, including the mass-size-shape-AMR relationships [21]. IMPACT's range of validity was also extended to lower energy fragmentation events to enable modelling of sub-catastrophic collisions and explosions. As additional data becomes available refinements to the model will continue.

5.3 SOCIT and DebriSat

Using a target with a realistic distribution of materials is critical for generating representative results for debris physical parameters. One of the main outputs from the SOCIT test was detailed measurements of the characteristics of the 100 largest fragments. In addition, sieving was done of samples of the smaller fragments to get numbers of fragments binned by size. This data has been used in the development of both SSBM and IMPACT, but as the demands of more detailed debris evolution and lethality modeling developed, the limitations of the SOCIT data became apparent in terms of the quantity and level of detail in the data. Additionally, over the last quarter century the materials used to make satellites and upper stages have changed.

These limitations and the needs of the fragmentation models drove a number of the choices made in the development of the DebriSat experiments. Because of the need to realistically represent the material composition of a satellite, a significant amount of effort was put into designing each of DebriSat's sub-systems to use materials and distribution and quantities of materials that would be representative of actual LEO satellites. Aerospace Corporation experts were consulted for each satellite sub-system to determine the more representative components and materials to use. Data on the construction of more than 100 satellites was used to determine a representative distribution of mass between the satellite sub-systems. The two efforts resulted in DebriSat's material composition having a wide spread of representative materials in approximately the proportions that would be expected for an actual satellite.

Research in the years since the SOCIT test has shown that small fragments can cause damage to satellites and their sub-systems. Because of this it has become more important to understand the characteristics of these small fragments, both in terms of how their physical characteristics will affect their ability to cause damage and to better understand how they are generated and how their orbits evolve, and to more accurately model the small fragment debris environment. This need for better data drove the DebriSat requirement to measure the physical characteristics of debris objects down to 2 mm. It has been observed that the distributions of physical characteristics of fragmentation debris are related to the material properties of the constituent materials. To better understand these distributions, both as a function of different material and in aggregate for satellites as a whole, it is necessary to have detailed information on the physical properties of large numbers of fragments of different materials individually as well as aggregate distributions over an entire set of materials that might

represent an actual satellite. This need has driven the DebriSat requirement for the detailed physical characterization of a large percentage of the debris fragments collected and the motivation for recoding information such as material.

5.4 DebriSat Data Usage

One of the major focuses of DebriSat data acquisition is the detailed and comprehensive characterization of debris fragment properties. This data will be used to improve the modeling of the relationships of these physical characteristics to each other and to generate representative distributions of such parameters as fragment mass, shape, size, and AMR. This information will be determined from DebriSat data in several ways.

The processing of DebriSat fragments includes not only the measurement of dimensions and mass but also the identification of the primary material of which the fragment is composed. This enables the segregation of fragments by material in order to explore differences in the mass, size, shape, and AMR distributions of fragments of different materials. It has been observed that the physical characteristics of fragments are a function of material and some initial efforts have been made to include these variations in fragmentation models to more effectively represent debris from objects of different compositions. Existing data has not been of sufficient detail and quantity to enable a more detailed development of material-dependent size, mass, number and AMR distributions or to expand the modeled materials to cover all of those commonly used in spacecraft construction. The quantity and material variety of the DebriSat fragments will enable this additional level of modeling fidelity.

DebriSat itself, at 56 kg, was sufficiently large to produce fragments that would have been large enough to track had the collision event occurred in orbit. These fragments and more generally, the ones a few centimeters and larger, provide a link between the fragments observed in on-orbit breakup events and those recreated in the DebriSat test series. Once measurements of the physical characteristics of these large DebriSat fragments have been completed it will be possible to compare the characteristics of these fragment distributions to those observed in on orbit breakups. Consistency in characteristics within the errors of measurements and differences between events will provide confirmation that the level of fidelity of the DebriSat tests was sufficient to provide a good representation of real-world breakups. It will also increase confidence that the characteristics of the smaller DebriSat fragments will provide a good representation of the corresponding results of on-orbit collisions where direct measurements have not been possible.

The high percentage of recovered mass anticipated from the DebriSat fragment collection process will enable a much more detailed examination of fragment number versus mass and number versus size distributions than has been possible with previous tests. In examinations of on-orbit collision events a roll-off from the expected power law distribution of cumulative fragment numbers versus mass or size can be seen as the limit of the SSN sensor sensitivity is approached. Previous ground tests indicate that this roll-off is an artifact of the increasing number of fragments that are missed by the tracking system rather than an actual decrease in the number of fragments below that predicted by the power law. Within the data from previous ground tests, such as SOCIT, there is also a roll-off at a lower value that is suspected of being caused by the incompleteness in fragment recovery. As with the on-orbit case, the more complete process of fragment recovery for the DebriSat test should enable a better understanding of actual versus artificial divergences from the expected power law distributions.

One of the debris fragment characteristics recorded is the fragment color. This can be used to assist in identifying the material from which the fragment was made. Additionally, the aluminum components in different sections of DebriSat were anodized in different colors. The color of fragments of these components, which is retained through the collision, can be used to identify the origins of subsets of the fragments within the original DebriSat structure. This will enable the examination of fragmentation characteristics of different known structures and at different locations and distances relative to the collision point of the projectile on DebriSat.

5.5 Damage Equations

Fragment physical characteristics, including shape and density, can play a significant role in determining the damage caused by these fragments when they impact satellites and other space structures. The distributions of fragment dimensions, shapes, and bulk densities as a function of material will enable identification of the most common density and shape characteristics for different classes of materials. These most common fragment characteristics can be used to focus damage assessment testing and modeling on the most likely types of debris to be encountered by satellites in on-orbit collisions with small fragments. Given the added difficulty in the testing and modeling of shape effects on collision damage, DebriSat data-based choices on where to focus the efforts

can maximize the correlation between test parameters and what is encountered on-orbit.

Shape-dependent effects are recognizable when examining the *in situ* record of impacts on returned surfaces and, by inference, even a cursory examination of the shapes of fragments generated in ground-based laboratories. These effects are notoriously difficult to replicate in the hypervelocity impact laboratory. However, the need to better estimate damage and risk and the quest for improved shielding provides the motivation for incorporation of shape effects into an evolved SSBM.

The ODPO has sponsored an initial investigation using a standard hydrocode to model the impacts of a set of spheroids, due to the simplicity of describing them by a single shape parameter. These have been compared with HVI testing with a limited degree of success. ODPO is also initiating studies on the number of parameters needed to characterize the six DebriSat shape categories and to describe their impact attitude with respect to a target surface. In addition, the manner by which these factors or functions are to be included in ballistic limit equations (BLEs) for all categories and all attack attitudes requires attention, as only simple shapes at 0° attack attitude and normal incidence have been validated in a conservative sense. For example, Schäfer, *et al*. [22] describe a course of research using ellipsoids described by a single shape parameter, f, the parameter's incorporation into a Cour-Palais/Christiansen BLE, and programs of HVI testing and numerical simulations to validate the modified BLE form. In this relatively simple case, the BLE required not only the shape parameter f but also five additional fit parameters to yield a reasonable fit. Significant work, theoretical, computational, and in the HVI laboratory, remains to be done.

6 SUMMARY

A historical overview of the DebriSat project was presented from the design phase that started in 2009, which was based on a key laboratory-impact test, SOCIT, a 1960's era Transit satellite that provided the foundation for the existing breakup models used by NASA and the DOD. The DebriSat characterization process was outlined that included prepping, extraction, and acquiring measurements on all fragments down to 2 mm in size. The focus for 2017 is two-fold: 1) validate the algorithm used to directly measure the third dimension (height) in the 2D imager and 2) complete the calibration in the 3D imaging system. Both of these systems are scheduled to be in operation well before the end of 2017. By the end of September 2017, a test plan will be defined for updating the current radar-based SEM and generating an optical-SEM using optical and radar facilities on a subset of selective fragments from DebriSat. Lastly, as sufficient quantities of the data become available the information will be used to update the breakup models.

7 REFERENCES

1. Liou, J.-C. et. al. (2014). Successful Hypervelocity Impacts of DebrisLV and DebriSat. *Orbital Debris Quarterly News***18**(3), pp3-6.
2. Liou, J.-C.. (2009). An Update on Recent Major Breakup Fragments. *Orbital Debris Quarterly News* **13**(3), pp5-6.
3. Werremeyer, M. (2013). Design of Sub-systems for a Representative Modern LEO Satellite, Dissertation, University of Florida.
4. Clark, S. (2013). Design of a Representative LEO Satellite and Hypervelocity Impact Test to Improve the NASA Standard Breakup Model, Dissertation, University of Florida.
5. Rivero, M., et al. (2016). DebriSat Fragment Characterization System and Processing Status, 67th International Astronautical Congress, Guadalajara, Mexico.
6. Rivero, M., *et al*. (2015). Characterization of Debris from the DebriSat Hypervelocity Test, International Astronautical Congress, Jerusalem, Israel.
7. Mulrooney, M., *et al*. (2008). An Investigation of Global Albedo Values, *Proceedings of the 2008 AMOS Technical Conference*, Wailea, Maui, HI.
8. Barker, E.S., *et al*. (2004). Analysis of Working Assumptions in the Determination of Populations and Size Distributions of Orbital Debris from Optical Measurements,. *Proceedings of the 2004 AMOS Technical Conference*, Wailea, Maui, HI.
9. Knott, E., *et al* (2004)*., Radar Cross Section*, 2nd Edition, SciTech Publishing, Inc. pp.64.
10. Hess, D. W. (2008). Introduction to RCS measurements, Antennas and Propagation Conference, pp37-44.
11. Skolnik, M.. (2001). *Introduction to Radar Systems*, 3rd Edition, McGraw-Hill, pp5-6, 50, 52.
12. Xu, Y., *et al.* (2005a). A Statistical Size Estimation Model for Haystack and HAX Radar Detections, IAC 2005.

14. Nathanson, F., *et al.* (1999). *Radar design principles: signal processing and the environment*, SciTech Publishing, pp.149-150.

15. Skolnik, M.. (2008). Radar Handbook, Edition 3, pp.629-630.

16. Xu, Y., *et al.*(2005b). A Bayesian Approach of Size Estimation for Haystack and HAX Radar Cross Section Observations, *Orbital DEbris Quarterly News*, **9**(2), pp5-6.

17. Johnson, N.L., *et al*.. (2001). NASA's New Breakup Model of EVOLVE 4.0. *Adv. Space Res*. **28**(9), pp1377-84.

18. Sorge, M., Mains, D. (2016). IMPACT Fragmentation Model Developments. *Acta Astronautica*.

19. Krisko, P.H., Horstman, M., and Fudge, M.L. (2008). SOCIT4 collisional-breakup test data analysis: with shape and material characterization. *Adv. Space Res.* **41**(7), pp1138-46.

20. Krisko, P.H., *et al*. (2008). Material Density Distribution of Small Debris in Earth Orbit, IAC-08.A6.2.1.

21. Sorge, M. E., Mains, D.L. (2014). IMPACT Fragmentation Model Improvements, AIAA 2014-4228.

22. Schäfer, F., Hiermaier,S., and Schneider, E. (2003). Ballistic Limit Equation for the Normal Impact of Unyawed Ellipsoid-shaped Projectiles on Aluminum Whipple Shields, IAC-03-IAA.5.3.06.